JOURNAL OF MATERIALS SCIENCE 35 (2000) 4477–4484

Process and wear behavior of monolithic SiC and short carbon fiber-SiC matrix composite

C. P. JU, C. K. WANG, H. Y. CHENG, J. H. CHERN LIN
Department of Materials Science and Engineering, National Cheng-Kung University, Tainan, Taiwan, R.O.C.
E-mail: cpju@mail.ncku.edu.tw

The process and wear behavior of monolithic SiC and 10 vol. % short carbon fiber-SiC matrix (C-SiC) composite have been studied. The results indicate that, among ethyl alcohol, acetone, *n*-hexane and *n*-octyl alcohol, *n*-octyl alcohol was the most effective dispersing agent in dispersing both SiC powder and short carbon fiber. Among AlN, Al_2O_3, B_4C, graphite, AlN/B_4C, AlN/graphite, B_4C/graphite and Al_2O_3/B_4C, the most effective sintering aid for the fabrication of SiC and C-SiC composite was a mixture of 2 wt% AlN and 0.5 wt% graphite. The monolithic SiC hot-pressed at 2100°C exhibited higher density but lower flexural strength than those hot-pressed at 2000°C due to a grain growth effect. For the C-SiC composite, both density and strength of the composite hot-pressed at 2100°C were generally higher than those hot-pressed at 2000°C. The density and strength of C-SiC composite were lower than those of monolithic SiC under the same hot pressing conditions due to a higher porosity level in the composite. When monolithic SiC slid against C-SiC composite, the weight losses of SiC and the composite were each less than that of self-mated SiC or self-mated C-SiC. In the self-mated SiC tribosystem, a mechanically stable film could not be established, resulting in an essentially constant wear rate. When sliding against C-SiC, a thin, smooth and adherent debris film was quickly formed on the SiC surface, resulting in a lower wear.

1. Introduction

Silicon carbide has been used in a variety of industries because of its many excellent properties, such as hardness, corrosion and oxidation resistance, and high temperature mechanical properties [1, 2]. When wearing against itself or other ceramics, SiC has generally exhibited rather high friction coefficients, typically in the range of 0.5–0.8 [3–5], except for those sliding in water or under other lubricated conditions. [6]

From their pin-on-disc sliding tests (normal load: 30–50 N; sliding velocity: 2 mm/s) of SiC/SiC couple, Takadoum *et al.* [3] found that the tribological behavior was sensitive to the sliding distance and relative humidity. In 50% humidity environment, both friction coefficient and wear rate were high in the initial stage due to the formation of abrasive wear particles. Repeated sliding led to compaction of such particles, that formed a protective debris layer, causing friction and wear to rapidly decreased after a critical distance. In the low relative humidity (20%) environment, however, this phenomenon was not as obvious. [4] At much higher sliding speeds (2.0 and 4.0 m/s), Blomberg *et al.* [5] found that the friction and wear behavior of their self-mated siliconized SiC was largely dependent on sliding velocity and load (10 and 80 N). At the sliding speed of 4.0 m/s, the friction coefficient increased with load, while at the lower speed (2.0 m/s), the friction coefficient decreased with load. The same authors also found that a passive tribo-oxidation process occurred at low loads and was characterized by the extensive formation of SiO_2. Under severe conditions, an active tribo-oxidation regime was defined, that was featured by the formation of SiO.

To evaluate the effectiveness of lubrication of carbon fiber incorporated in SiC, a pitch-based carbon fiber (10 vol. %)-silicon carbide matrix (C-SiC) composite was fabricated in this study. The selection of the high modulus pitch-based fiber was based on its highly graphitic nature (the basal planes are highly aligned and plastic deformation is more easily to occur). The continual supply of "self-regenerative" carbon lubricant from the composite is one major advantage over the common application of a thin layer of graphite powder on ceramic surface as a solid lubricant by various techniques [7, 8].

2. Experimental procedure

Types and selected properties of the various raw materials used in this study are listed in Tables I–III. The α-SiC powder (Fig. 1a) had an average particle size of 0.5 μm, with the largest about 4 μm, as measured by a laser particle analyzing system (LPA-3000/3100, Otsuka Electronics Co., Tokyo, Japan). The short carbon fibers (Fig. 1b,c) with lengths of 1–2 mm and aspect ratios of >100 used for the fabrication of C-SiC

TABLE I Powders used in the study

Powder	Particle size	Purity	Source
α-SiC	$<4\,\mu$m	>98.5%	HCST, A10
Al_2O_3	avg. $1\,\mu$m	>99.0%	Brand A-32
AlN	avg. $1\,\mu$m	>99.0%	HCST
B_4C	$<10\,\mu$m	>99.5%	HCST
Graphite	$<2\,\mu$m	>99.9%	CERAC, G-1059

TABLE II Chemical composition of SiC powder used in the study

	Free Si	C	O	Fe	Al	Ca	others
Max. wt%	0.1	29.5–30.5	1.1	0.03	0.03	0.01	0.05

*Data provide by Hermann C. Starck, Inc. (HCST) of USA.

TABLE III Carbon fiber used in the study

Tensile strength	Tensile modulus	Density	Diameter
2960 MPa	586 GPa	2.16 g/cm^3	7–8 μm

*Data provide by Petoca Inc. of Japan.

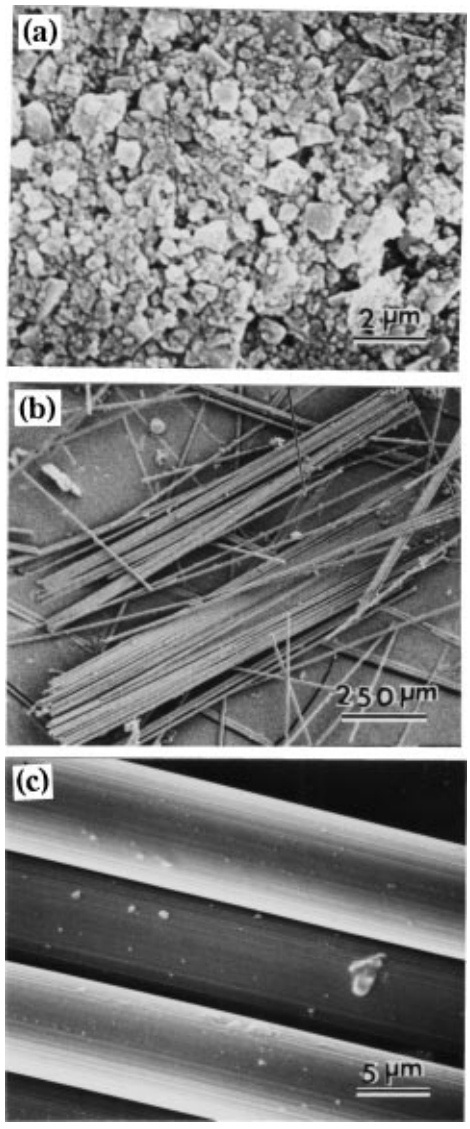

Figure 1 SEM micrographs of as-received SiC powder (a) and carbon fiber (b, c) used in the study.

composite were chopped from a high modulus, high strength mesophase pitch-based continuous fiber (Petoca HM60-2K-723, Japan).

The sintering aids tested in this study for the fabrication of monolithic SiC as well as C-SiC composite included AlN, Al_2O_3, B_4C, graphite and some of their combinations in different ratios. Such solutions as ethyl alcohol, *n*-octyl alcohol, acetone and *n*-hexane were tested for the dispersion of the short carbon fibers. The dispersing ability of such solutions was evaluated by the 24-hour settling height of 50 mg fiber ultrasonically dispersed (80 W, 2 min) in a 28 mm dia. test tube containing 40 ml dispersing solution.

A High Multi 5000 (Fujidempa Kogyo Co., Ltd, Osaka, Japan) vacuum/inert hot pressing system was used to fabricate the SiC and C-SiC composite. Peak temperatures of 2000 and 2100°C and peak pressure of 25 MPa in 1 atm argon atmosphere were used throughout the study. For the fabrication of monolithic SiC, appropriate amounts of SiC and sintering aid powders were ball-mill (using SiC balls) mixed in ethyl alcohol, fast dried, ground into powder, and mixed again with a small amount of ethyl alcohol to form a thick slurry. This slurry was press-molded into round disks of 5.0 cm in diameter and desirable thicknesses, followed by drying at 100°C for 6 hours. The dried disks were ready for the final hot pressing.

To fabricate the C-SiC composite, appropriate amounts of short carbon fibers and SiC powder with sintering aid were ultrasonically dispersed (80 W, 2 min) in *n*-octyl alcohol and acceleratively dried on a heated stainless steel plate enclosed in an evacuated (mechanically pumped) container to make C-SiC "prepreg" fragments (Fig. 2). Such C-SiC fragments were mixed with a small amount of ethyl alcohol to form a thick slurry, that was subsequently press-molded, dried and hot pressed.

The densities of hot-pressed SiC and C-SiC were measured using the ASTM C373-72 method [9]. Four-point bending tests (following ASTM F417-78 method) were performed using an Instron 8562 system. A deflection speed of 0.5 mm/min was used for all tests. The surfaces of tested specimens were mechanically polished to 1 μm level. All strength data were averages of five tests for each condition. With the same four-point bending setup, the fracture toughness (K_{1C}) measurement was carried out using the

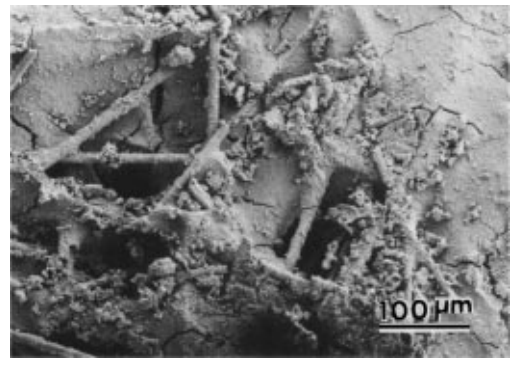

Figure 2 SEM micrograph of C-SiC prepreg fragment.

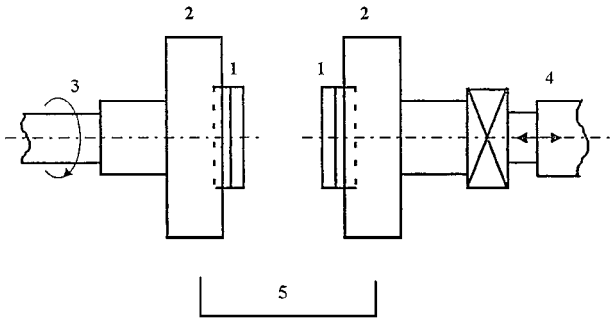

1. specimen 2. specimen holder 3. rotating shaft
4. to loading system 5. debris collector

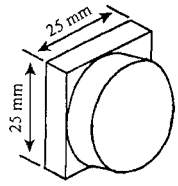

Figure 3 Wear tester and specimen specification.

single edge notched beam (SENB) technique. A notch of width (a) of 0.4–0.42 mm and depth (h) of 1.1–1.2 mm was introduced into specimens for the measurement. The toughness was calculated using the equation [10], $K_{1C} = \sigma Y a^{1/2}$, where $Y = 1.99–2.47(a/h) + 12.97(a/h)^2 - 23.17(a/h)^3 + 24.80(a/h)^4$. Averages of five tests were taken for each condition.

Dry sliding wear tests were performed at room temperature in air using a homemade disc-on-disc wear tester (Fig. 3). A constant speed of 60 rpm (equivalent to an average linear speed of 0.04 m/sec) and normal pressure of 0.85 MPa (420 N) were used for all tests. All SiC and C-SiC specimens for wear testing were hot-pressed at 2000°C and 25 MPa. Prior to testing, the specimen surfaces were flattened using a #500 diamond wheel. All the measured weight loss data were averages of five tests for each condition. A Nikon FM2 optical camera (Tokyo, Japan) was used to photograph the sequential variation in overall surface morphology, while a S-2500, Hitachi scanning electron microscope (SEM) (Tokyo, Japan) was used to examine the worn microstructure in more detail.

3. Results and discussion

3.1. Process and properties

Okuyama [11] has shown that such dispersing agents as ethyl alcohol, *n*-octyl alcohol, acetone and *n*-hexane are effective in dispersing SiC powder. In the present study, the same solutions were tested, using the method described in Experimental Procedure, to disperse short carbon fibers. Results of a series of tests identified the most effective dispersing agent for both short carbon fibers and SiC powder to be *n*-octyl alcohol. This agent was then used for the fabrication of all C-SiC specimens.

A variety of sintering aids, such as B [12], C [12], B_4C [13], Al_2O_3 [14], AlN [15], Al [16] and Fe [16, 17], have been used in the literature for fabrication of monolithic SiC. As mentioned in Experimental Procedure, the sintering aids first tested in this study for the fabrication of SiC as well as C-SiC composite included AlN, Al_2O_3, B_4C and graphite. Evaluation of performance of the various sintering aids was based on the various properties, as shown in Table IV, of the final hot-pressed products. Through a series of tests, the best formula was identified to be a mixture of 2 wt% AlN and 0.5 wt% graphite. Although there already existed 10 vol% carbon fiber in the composite, the addition of graphite powder in the matrix largely assisted the sintering process of SiC matrix. This formula was then used throughout the subsequent study for the fabrication of SiC as well as C-SiC composite. Fig. 4 is an example showing a

TABLE IV Effect of sintering aid on properties of hot-pressed SiC and C-SiC

Sintering aid	C-fiber (vol%)	Temperature (°C)	D_b/D_{th} (%)	δ_f (MPa)	H_v (MPa)	K_{1C} (MPam$^{-1/2}$)
1.5wt%Al_2O_3	0	2000	91.3	327 ± 18		
2.05wt%Al_2O_3	0	2000	90.6	253 ± 13		
2.5wt%Al_2O_3	0	2000	91.6	319 ± 14		
0.5B_4C + 2.05wt%Al_2O_3	0	2000	91.5	222 ± 14		
1.0 wt%B_4C	0	2000	86.8	296 ± 32		
2.0 wt%B_4C	0	2000	89.6	273 ± 16		
3.0 wt%B_4C	0	2000	87.5	285 ± 15		
0.5 C + 1.0 wt%B_4C	0	2000	90.5	283 ± 12		
1.5wt% AlN	0	2000	94.2	388 ± 38		
2.0wt% AlN	0	2000	98.6	378 ± 25		
2.5wt% AlN	0	2000	96.5	390 ± 21		
0.5 B_4C + 2.0wt% AlN	0	2000	98.0	204 ± 20		
0.5 C + 2.0wt% AlN	0	2000	98.8	463 ± 22	3065 ± 207	4.87 ± 0.32
0.5 C + 2.0wt% AlN	0	2100	99.1	369 ± 24	2612 ± 126	
0.5 C + 2.0wt% AlN	5	2000	94.8	286 ± 18	2536 ± 237	4.75 ± 0.22
0.5 C + 2.0wt% AlN	5	2100	96.9	282 ± 16	2242 ± 248	
0.5 C + 2.0wt% AlN	10	2000	93.8	187 ± 20	2361 ± 146	4.13 ± 0.15
0.5 C + 2.0wt% AlN	10	2100	96.1	246 ± 16	2150 ± 132	
0.5 C + 2.0wt% AlN	15	2000	90.8	91 ± 14	2320 ± 142	3.48 ± 0.18
0.5 C + 2.0wt% AlN	15	2100	94.5	180 ± 18	2164 ± 113	

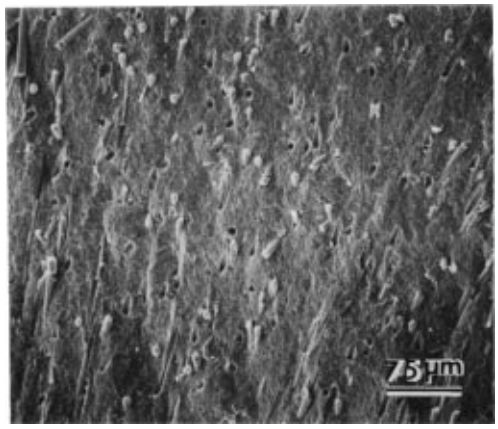

Figure 4 SEM fractograph of C-SiC composite.

quite uniform fiber distribution in a composite specimen comprising 10 vol% fiber, that was hot-pressed at 2000°C using *n*-octyl alcohol as dispersion agent and 2 wt% AlN/0.5 wt% graphite as sintering aid. The effect of sintering aid on density and flexural strength of hot-pressed SiC and C-SiC is summarized in Table IV. As shown in the table, the hot-pressed monolithic SiC at 2000°C with AlN as sintering aid had a higher density (98.6% of theoretical) and flexural strength (about 380 MPa) than those with Al_2O_3 or B_4C. As a comparison, a density of only 64.2% was obtained without any sintering aid under the same condition.

As 0.5 wt% graphite was added as a second sintering aid component, the density and strength of SiC further increased. For example, using 2 wt% AlN/0.5 wt% graphite as sintering aid (the most effective sintering aid in this study), a SiC hot-pressed at 2000°C with a density of 98.8 g/cm^3 and flexural strength of 460 MPa was fabricated. Fig. 5 clearly shows that SiC porcessed with the sintering aid of 2 wt% AlN/0.5 wt% graphite has less porosity than using other sintering aids.

When SiC was hot-pressed at 2100°C with the same two-component sintering aid, a density of higher than 99% of theoretical was achieved, although the flexural strength became lower (about 370 MPa) due to a grain growth effect (Fig. 6). Nevertheless, for C-SiC composite, both density and strength of the composite hot-pressed at 2100°C were always higher than those hot-pressed at 2000°C. Obviously, the grain growth effect was largely suppressed due to the presence of fibers in the composite.

As indicated in Table IV, both density and flexural strength of the C-SiC composite were lower than those of monolithic SiC under the same hot pressing conditions. Obviously, the presence of the short fibers did not strengthen, but weaken the material using the present relatively simple fabrication method. SEM examination indicated a higher porosity level in the composite than in the monolithic SiC. In addition that the presence of carbon fibers has caused SiC harder to sinter, the large

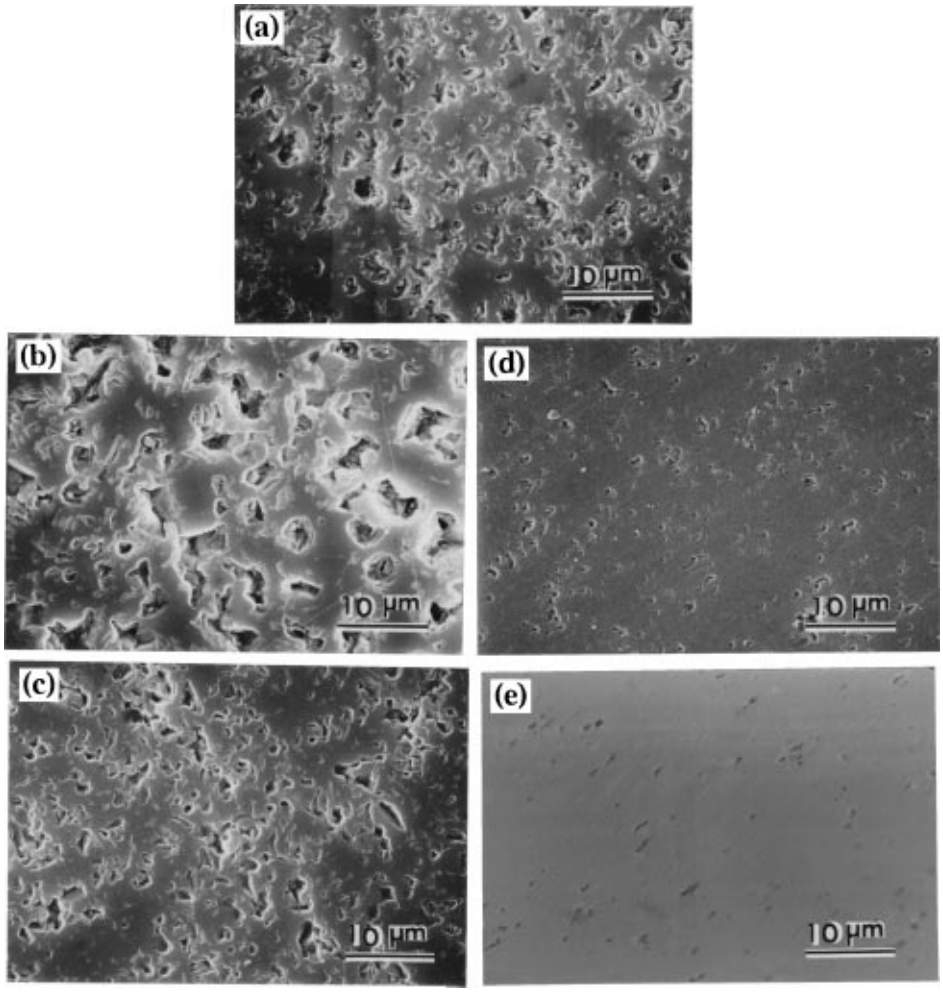

Figure 5 SEM micrographs of polished SiC using different sintering aids. (a) 2 wt% B_4C, 2000°C; (b) 2 wt% Al_2O_3, 2000°C; (c) 2 wt% AlN, 2000°C; (d) 2 wt% AlN + 0.5 wt% graphite, 2000°C; (e) 2 wt% AlN + 0.5 wt% graphite, 2100°C.

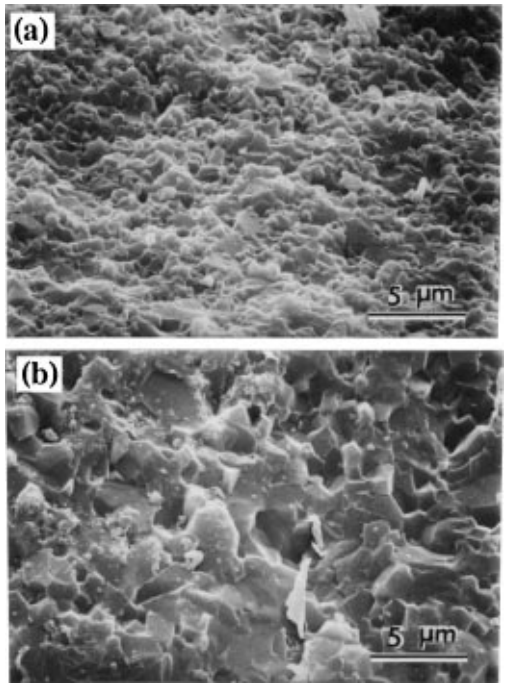

Figure 6 SEM fractographs of SiC hot pressed at 2000°C (a) and 2100°C (b).

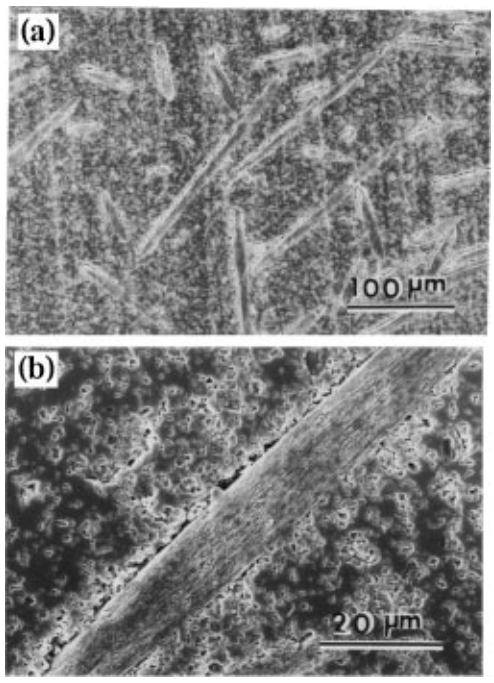

Figure 7 SEM micrographs of polished C-SiC using 2 wt% AlN + 0.5 wt% graphite as sintering aid at 2000°C. (a) ×250; (b) ×1500.

difference in coefficient of thermal expansion (CTE) between SiC (about 4.5×10^{-6}/°C) and the high modulus fiber, particularly in the fiber axis direction (near zero CTE), could have induced significant residual tensile stress at fiber-matrix interface when the composite was cooled down from high temperatures. Indeed, in the present composite, fibers were frequently observed to be more or less debonded from surrounding SiC (Fig. 7). This weak interface might also be accountable for the reduced strength of the composite. This is one of the reasons that many advanced C-SiC composites are fabricated using continuous woven fibers in-

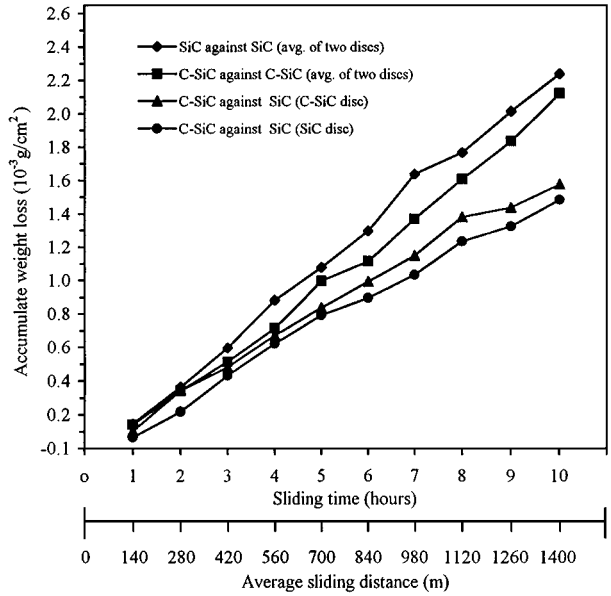

Figure 8 Weight losses of SiC and C-SiC with sliding time/sliding distance.

filtrated/densified by chemical vapor infiltration (CVI) processed at much lower temperatures [18].

3.2. Wear behavior

Fig. 8 represents accumulated weight losses with time of monolithic SiC and C-SiC composite sliding against each other and against themselves. For self-mated SiC, the weight loss data were averages of both disks (stator and rotor). For SiC against C-SiC, however, weight losses of the two disks were measured separately. The results showed that the weight loss of SiC sliding against itself was the largest among the four cases. When SiC slid against C-SiC composite, the weight losses of SiC and the composite were each less than that of self-mated SiC or self-mated C-SiC. Their differences increased with sliding time and, after 10 hours, the weight loss of SiC sliding against C-SiC (the smallest) became less than that of self-mated SiC (the largest) by 35%.

To explain the present wear data, it seems that at least two material factors should be considered: 1) relative hardness and strength, and 2) whether a carbon lubricant is present. Effect of the first factor was readily seen from the fact that SiC was consistently less worn than the weaker and softer counterpart composite. Effect of the second factor is justified by the fact that SiC was always less worn when sliding against the composite than against itself. The data in Fig. 8 clearly indicates the effectiveness of the presence of carbon in the tribosystem in reducing the wear of SiC. It is interesting to note that, despite the large difference in flexural strength between SiC and C-SiC, the two materials were both less worn when sliding against each other. It would also be interesting to know whether further improvement in wear resistance for this SiC-composite tribosystem can be achieved, should density and strength of the composite be improved using different fabrication processes.

Fig. 9 represents the sequential variation in surface/debris morphology of self-mated SiC. As shown in

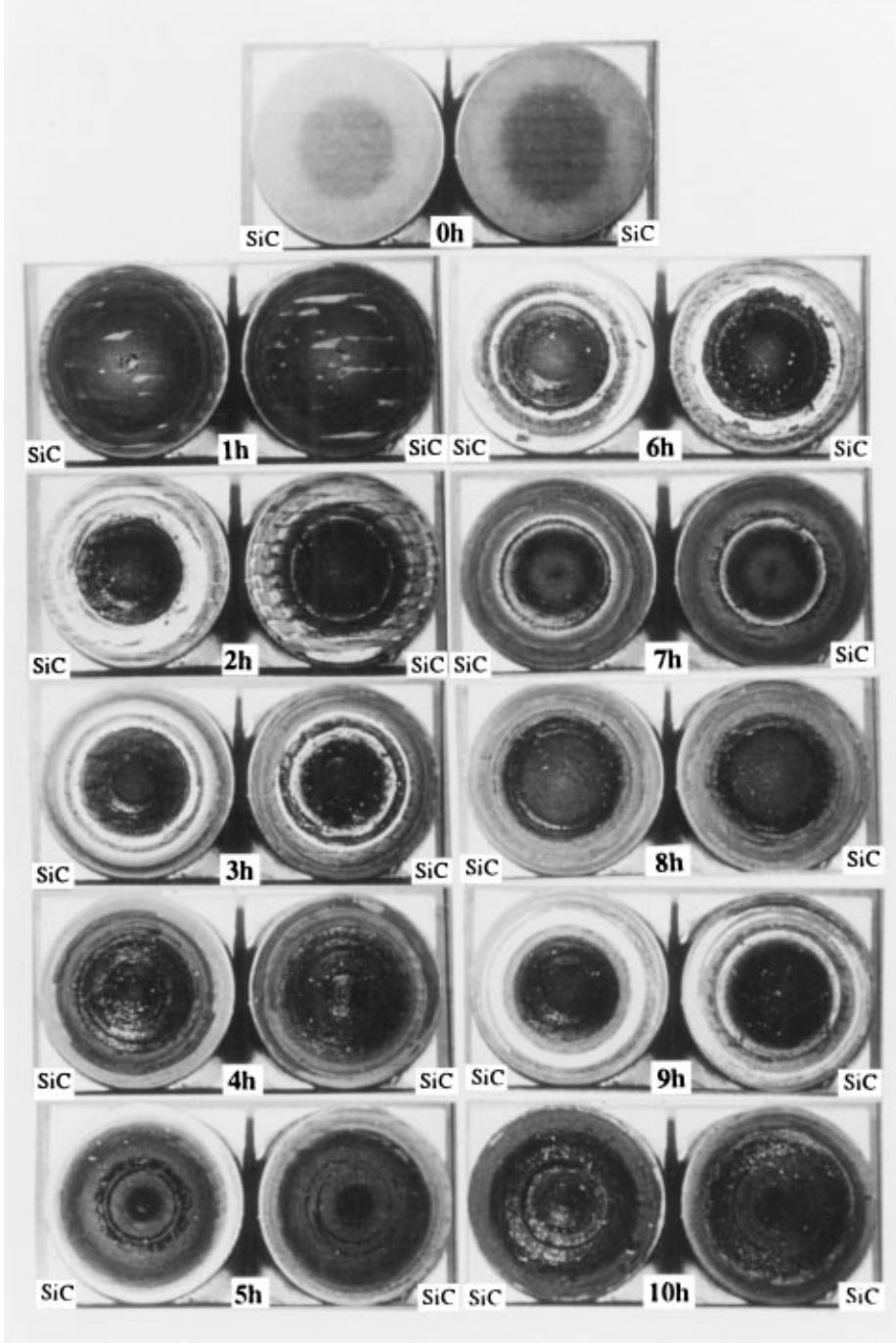

Figure 9 Sequential variation in worn surface morphology of SiC sliding against SiC.

the photographs, the SiC specimen essentially underwent a mechanical polishing (wear-in) process in the first sliding hour. During the second hour, patches of wear debris film were generated. This debris film was loosely attached to the surface, while portions of it had readily broken off the surface. After 4 hours, the debris film was entirely disrupted and transformed into a powdery type of debris. A major portion of this powdery debris escaped the wear surface, as seen on the 5-hour specimen, contributing to weight loss. After 6 hours, the first type of film debris was developed again. Similar to its initial formation, the film was loosely attached and was easily disrupted. Due to the rotation of specimens, partial disruption of the film resulted in band-like worn surface/debris morphology. Once disrupted, the film was quickly transformed into powder again, as described earlier. The 9-hour specimen showed that the debris morphological variation sequence, i.e., film formation, disruption into powder, and re-formation, started again. This repeated sequence indicated that a mechanically stable debris film could not be established in this self-mated SiC tribosystem, that resulted in an essentially constant wear rate, as shown earlier in Fig. 8.

Fig. 10 shows the sequential variations in surface/debris morphology of both SiC and its C-SiC counterpart, when the two slid against each other. Compared to that of self-mated SiC, the wear debris was formed more quickly in the SiC-composite tribosystem due to the lower hardness and strength of the composite. After 1 hour of sliding, wear debris was readily observed. Unlike that observed on the self- mated SiC worn surfaces, the surface/debris morphologies of SiC and C-SiC were

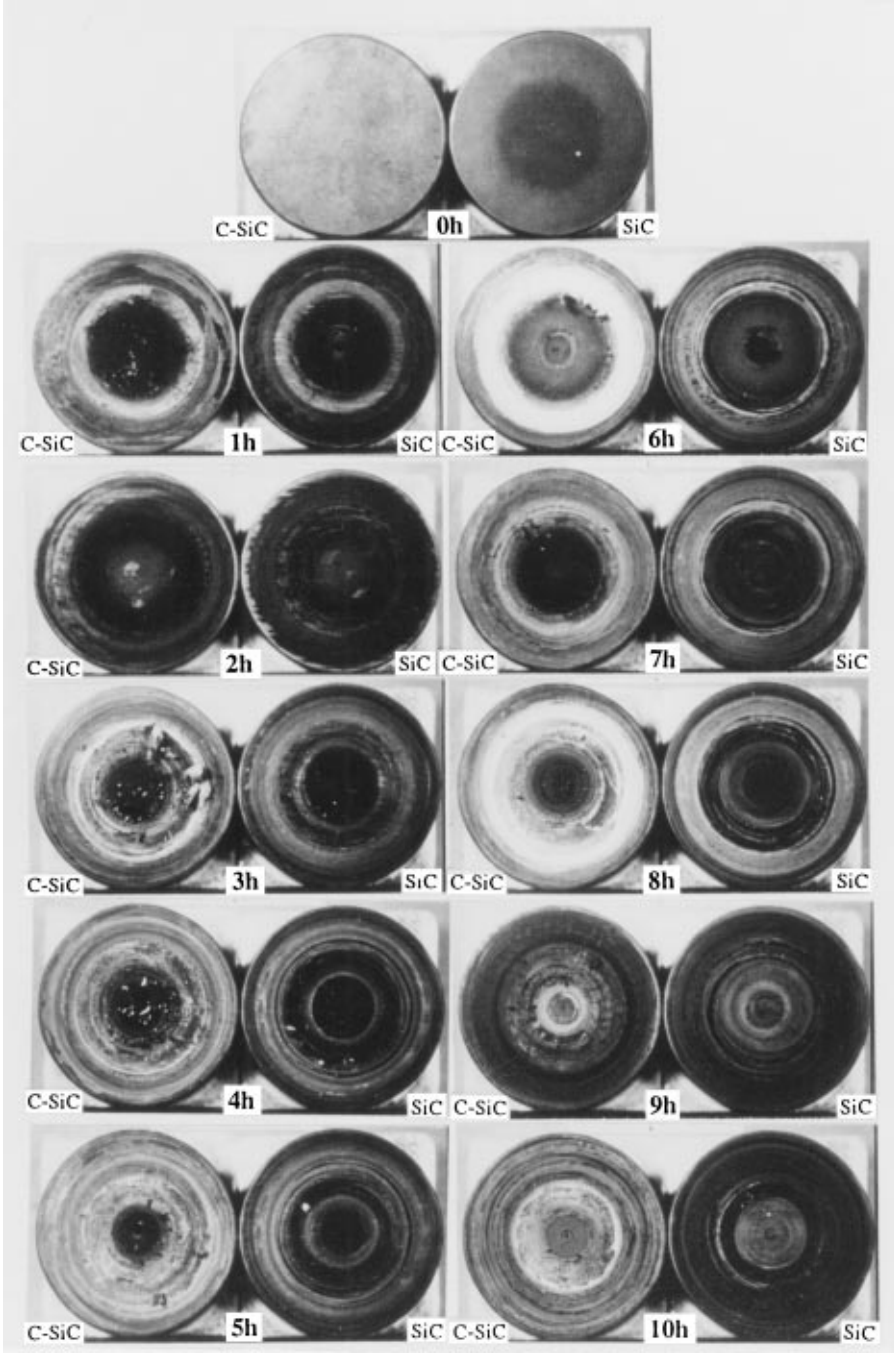

Figure 10 Sequential variations in worn surface morphology of SiC and C-SiC sliding against each other.

significantly different. On the composite surface, a massive debris film was formed and disrupted quickly in the first few hours. After roughly 5 hours, a more adherent debris film started to cover the worn surface. The development of this film seems to explain the gradual reduction in wear rate of the composite.

On the other hand, on the SiC surface, a thinner, adherent debris film was quickly formed that, under the present sliding condition, was never massively disrupted throughout the test. Obviously the presence of carbon has played a critical role in the formation of the more stable debris film. The development of this more stable (probably also more lubricative) film helped slow down the wear rate, as shown in Fig. 8. Among all various worn surfaces, the worn surface of SiC, when sliding against C-SiC composite, was the most uniform, smooth and shiny, in addition to its most mechanical stability. This type of surface/debris morphology has resulted in the smallest weight loss, as mentioned earlier. The reason why C-SiC composite had a larger weight loss than that of SiC, when the two specimens slid against each other, is believed due to the softer and weaker (with more inherent porosity) nature of the composite. Nevertheless, the continual supply of carbon from the composite very effectively helped bring down the wear of both materials, especially the SiC counterpart.

4. Conclusions

1. Among ethyl alcohol, acetone, *n*-hexane and *n*-octyl alcohol, *n*-octyl alcohol was the most effective dispersing agent in dispersing both SiC powder and short carbon fiber.

2. Among AlN, Al_2O_3, B_4C, graphite, AlN/B_4C, AlN/graphite, B_4C/ graphite and Al_2O_3/B_4C, the most effective sintering aid for the fabrication of SiC and C-SiC composite was identified to be a mixture of 2 wt% AlN and 0.5 wt% graphite.

3. Monolithic SiC hot-pressed at 2100°C exhibited higher density but lower flexural strength than those hot-pressed at 2000°C due to a grain growth effect. For C-SiC, both density and strength of the composite hot-pressed at 2100°C were always higher than those hot-pressed at 2000°C. The density and strength of C-SiC composite were lower than those of monolithic SiC under the same hot pressing conditions due to a higher porosity level in the composite.

4. When monolithic SiC slid against C-SiC composite, the weight losses of SiC and the composite were each less than that of self-mated SiC or self-mated C-SiC. After 10 hours, the SiC sliding against C-SiC composite was less worn than self-mated SiC by 35%.

5. In self-mated SiC tribosystem, the process of debris film formation, disruption and re-formation repeated and a mechanically stable film could not be established, resulting in an essentially constant wear rate. When SiC slid against C-SiC, a thin, smooth and adherent debris film was quickly formed on the surface, that was never massively disrupted throughout the test, causing wear to slow down.

Acknowledgement

The authors are grateful to National Science Council of Republic of China for support of this research under the contract NSC 82-0405-E006-341.

References

1. K. SUGANUMA, G. SASAKI, T. FUJITA, M. OKUMURA and K. NIIHARA, *J. Mater. Sci.* **28** (1991) 1175.
2. M. LANDON and F. THEVENOT, *Ceram. Int.* **17** (1991) 97.
3. T. TAKADOUM, Z. ZSIGA and C. R. CARMES, *Wear* **174** (1994) 239.
4. T. TAKADOUM, Z. ZSIGA, N. B. RHOUMA and C. R. CARMES, *J. Mater. Sci. Lett.* **13** (1994) 474.
5. A. BLOMBERG, M. OLSSON and S. HOGMARK, *Wear* **171** (1994) 77.
6. L. C. ERICKSON, A. BLOMBERG, S. HOGMARK and J. BRATTHÄLL, *Tribo. Int.* **26** (1993) 83.
7. A. GANGOPADHYAY and S. JAHANMIR, *Tribo. Trans.* **34** (1991) 257.
8. A. SKOPP, M. WOYDT, K. H. HABIG, T. KLUG and R. BRÜCKNER, *Wear* **169** (1993) 243.
9. "Standard test method for water absorption, bulk density, apparent porosity, and apparent specific gravity of fired whiteware products," 1984 Annual Book of ASTM Standards, vol. 15.02 C373 p. 182.
10. R. F. PABST, in "Fracture Mechanics of Ceramics, Vol. 2, Microstructure, Materials, and Applications," edited by R. C. Bradt, D. P. H. Hasselman and F. F. lange (Plenum Press, New York, 1974) p. 555.
11. M. OKUYAMA, *J. Am. Ceram. Soc.* **72** (1989) 1918.
12. S. PROCHAZKA and R. M. SCANLAN, *ibid.* **58** (1975) 72.
13. D. R. SECRIST, *ibid.* **47** (1964) 127.
14. F. F. LANGE, *J. Mater. Sci.* **10** (1975) 314.
15. W. RAFANIELLO, K. CHO and A. V. VIRKAR, *ibid.* **16** (1981) 3479.
16. R. A. ALLIEGRO, L. B. COFFIN and J. R. TIINKLEPAUGH, *J. Am. Ceram. Soc.* **39** (1956) 386.
17. B. W. LIN, M. IMAI, T. YANO and T. ISEKI, *ibid.* **69** (1986) C-67.
18. E. FITZER and R. GADPW, *Am. Ceram. Soc. Bull.* **65** (1986) 326.

Received 5 May 1997
and accepted 15 March 2000